S.O.S: Shape, orientation, and size tune solvation in electrocatalysis

Alessandra Serva, Simone Pezzotti

S.O.S: shape, orientation and size tune solvation in electrocatalysis

Alessandra Serva[1, a)] and Simone Pezzotti[2, b)]
[1)] *Sorbonne Université, CNRS, Physico-chimie des Electrolytes et Nanosystèmes Interfaciaux, PHENIX, F-75005 Paris, France*
[2)] *PASTEUR, Département de Chimie, Ecole Normale Supérieur, PSL University, Sorbonne Université, CNRS, 75005 Paris, France*

Current models to understand the reactivity of metal/aqueous interfaces in electrochemistry, e.g. volcano plots, are based on the adsorption free energies of reactants and products, which are often small hydrophobic molecules (such as in CO_2 and N_2 reduction).calculations, played a major role in the quantification and comprehension of these free energies in terms of the interactions that the reactive species form with the surface. However, also solvation free energies come into play in two ways: (i) by modulating the adsorption free energy together with solute-surface interactions, as the solute has to penetrate the water adlayer in contact with the surface and get partially desolvated (which costs free energy); (ii) by regulating transport across the interface, i.e. the free energy profile from the bulk to the interface, which is strongly non-monotonic due to the unique nature of metal/aqueous interfaces. Here, we use constant potential Molecular Dynamics to study the solvation contributions and we uncover huge effects of the shape and orientation (on top of the already known size effect) of small hydrophobic and amphiphilicsolutes on their adsorption free energy. We propose a minimal theoretical model, the S.O.S. model, that accounts for size, orientation and shape effects. These novel aspects are rationalized by recasting the concepts at the base of the Lum-Chandler-Weeks theory of hydrophobic solvation (for small solutes in the so-called volume-dominated regime)into a layer-by-layer form, where the properties of each interfacial region close to the metal are explicitly taken into account.

I. INTRODUCTION

Chemistry at electrified solid/liquid interfaces strongly depends on the way reactive species are adsorbed and solvated at the interface.[1–11] First, adsorption of reactants and desorption of products are the initial and last step of any electrocatalytic process, which regulate the transport of matter across the interface and are often rate-determining. Second, adsorption energy of reactants and products are used as descriptors in volcano analyses to assess the catalytic efficiency of a surface.

Adsorption free energies are commonly evaluated with the help of theory, by means of static calculations at the Density Functional Theory (DFT) level, which greatly advanced the field of electrocatalysis and even inspired in-silico design of electrode materials in some cases.[5–9,11–13] These calculations are performed either excluding the solvent molecules or treating them with implicit models, thus not taking into account the specific solvation properties of the interface. However, a growing number of experimental and theoretical studies highlighted that solvation properties at the interface play a major role in shaping the adsorption free energies, as well as in regulating the transport of reactive species across the whole interfacial region.[1–3,14–22] From a theoretical point of view, some of the solvation effects can be studied with the help of molecular dynamics (MD) simulations.[23–33] Taking the case of electrified metal/aqueous interfaces, recent works have shown that the peculiar organization of water molecules at the interface gives rise to solvation and adsorption behaviors that cannot be captured by existing solvation theories (generally developed for bulk systems), neither by implicit solvation models that are currently used in DFT calculations.[15,22,34] For example, we have recently shown that hydrophobic solvation at these interfaces follows different rules than in the bulk:[15,18] an additional free energy term must be considered, which accounts for the specific molecular arrangement of the interface, and which e.g. strongly modulates the size-dependence of hydrophobic solvation close to the electrode. However, if on the one side, tuning the interfacial solvation contribution opened interesting perspective for regulating electrochemical processes, on the other side, we currently lack the knowledge to exploit these avenues.

In the present work, we tackle this problem by studying the solvation contribution on a Au(100)/water interface with the aid of constant potential classical MD. We focus on the solvation of hydrophobic and amphiphilic molecules that are particularly relevant for electrocatalytic processes at metal/aqueous interfaces, such as for CO_2 reduction and alcohol oxidation. For such molecules, the solvation free energy ($\Delta\mu_v$) is dominated by the process of cavity formation (that must be carefully described in order for implicit solvation and microsolvation approaches to meaningfully reproduce the solvation behavior).The free energy of cavity formation depends on the probability that a cavity of the right size to host the solute is spontaneously formed in the liquid via fluctuations of the water density ($P_v(0)$):[35–39]

$$P_v(0) = e^{-\beta\Delta\mu_v} \quad (1)$$

where v is the volume of the cavity formed by the

[a)] Electronic mail: alessandra.serva@sorbonne-universite.fr
[b)] Electronic mail: simone.pezzotti@ens.psl.eu

molecule in water and $\beta = 1/k_BT$While until now the size dependence has been regarded in hydrophobic solvation theories/modelsas the most relevant effect on the free energy of cavity formation (with few exceptions[40,41]), we uncover here shape and orientation effects that exceed size-effects by order of magnitude. We show that this is due to how water density fluctuations evolve across the distinct water layers formed in contact with the metal, and we propose a minimal theoretical model, the S.O.S. model, that accounts for the effects of size, orientation and shape of small solutes. These novel aspects call for re-evaluating our understanding of interfacial solvation, and have interesting implications for electrocatalysis.

II. RESULTS AND DISCUSSIONS

A. Some background on interfacial structure and solvation

The molecular organization of metal/water interfaces has been investigated in a number of previous works (e.g. Refs. 15,19,34,42–47), and is illustrated in Fig. 1 for an Au(100)/water interface. The strong binding of water molecules to the metal leads to the formation of a hydrophilic interface (I1) between the metal and the water adlayer on top of it. The adlayer has a very ordered structure, maximizing both water-metal interactions and water-water H-Bonds. However, it retains only few spots for H-bonding with the adjacent water layer, behaving as if it were a hydrophobic surface. This leads to the formation of a second interfacial region (I2) between the two water layers, exhibiting some features typical of hydrophobic environments, e.g. enhanced fluctuations of the water density[15,34] and a spectroscopic feature in the THz range.[16,48] A third interfacial region (I3), similar to the topmost water layer in contact with a hydrophobic surface, is observed before reaching a bulk-like structure. Therefore, metal/water interfaces can be regarded as composed of several interfaces in series.

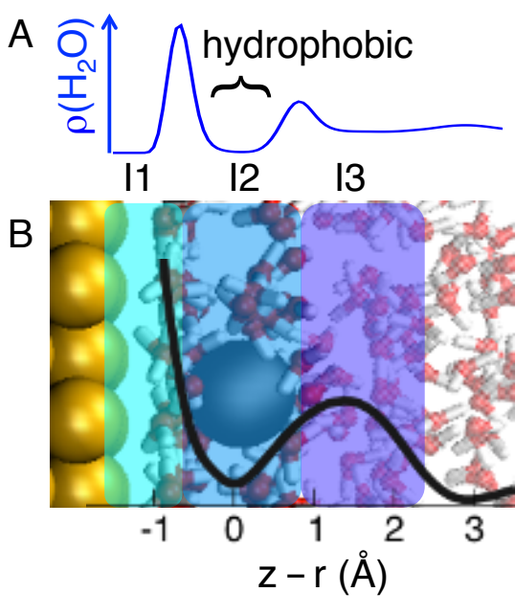

FIG. 1. **The Au(100)/water interface.** A) Water density profile in the direction perpendicular to the surface, as obtained from constant potential classical MD simulations. B) MD snapshot highlighting the 3 interfacial regions (I1, I2 and I3) formed close to the electrode, with I2 being a hydrophobic water-water interface. The black curve represents the free energy profile to bring an ideal spherical hydrophobe (i.e a cavity of r= 2.5 Å) from the bulk to the surface. The gray sphere at $z - r = 0$ Å shows the cavity in its more stable position within the I2 region.

This layering influences the free energy profile to adsorb hydrophobic/amphiphilic solutes (Fig. 1B), which is non-monotonic as it depends on how water density fluctuations evolve across I1-I3[15] (see eq. 1 and method section). In the following, we will show that such layering and the associated abrupt changes in density fluctuations are responsible for atypical effects of shape and orientation on the solvation at the interface.

B. Shape and orientation effects

We start our investigation by performing a simple theoretical experiment. We compute (see methods) the adsorption free energy for bringing three idealized solutes (i.e. cavities) of different shape or orientation but same volume from the bulk to their most stable location at the Au(100)/water interface (which is right after the I1 region for all solutes, see Fig. 2A for a sketch). As illustrated in the figure, for the shape we consider spheres and bricks, while for the orientation H-bricks and V-bricks, which longest edge is either parallel or perpendicular to the surface. The difference in shape and orientation modifies how the solute cavity is distributed among the interfacial layers. We then repeat the same experiment for different sizes, ranging from an equivalent radius (r) of 2.0 Å to 3.5 Å. For the bricks, the volume is increased by elongating the longest edge. This, for example, means that when increasing the volume H-bricks will remain mostly within the I2 region, while V-bricks will protrude into I3 and then into the subsequent bulk region. Cavities in this size-range are typically formed by small organic molecules such as CO, CO_2, CH_4, CH_3OH, as previously confirmed in e.g. ref. 15. The bricks, in particular, can be thought as an idealized approximation of linear molecules such as CO_2. The computed adsorption free energy values are plotted in Fig. 2B as difference with respect to the value in the bulk, $\delta\mu_v(z*)$, normalized by r^2 (in units of k_BT, with $\beta = 1/k_BT$). A negative $\delta\mu_v(z*)$ means a more stable solvation at the interface than in the bulk, i.e. favorable

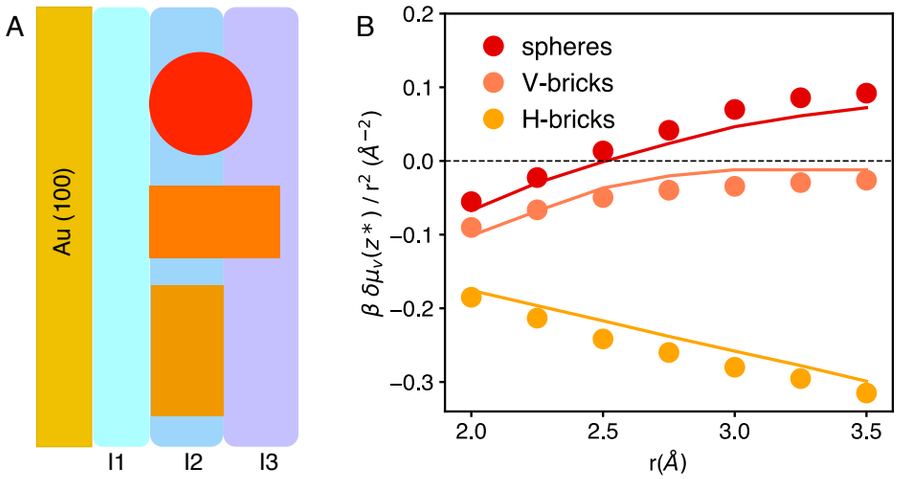

FIG. 2. **The atypically large shape and orientation effects at metal/water interfaces and the S.O.S. model.** A) Illustration of a theoretical experiment performed on three ideal hydrophobes (i.e cavities) of same volume but different shape/orientation: spheres (red), V-bricks (orange) and H-bricks (dark yellow), where H/V-bricks are horizontally and vertically lying cuboids.The shape/orientation changes the way the cavities spread among the interfacial I1-3 regions (highlighted in different blue shades). B) Adsorption free energy values obtained from the MD simulation for the three cavities as a function of increasing volume (i.e. increasing equivalent radius, r). The free energies, as a function of r, are reported as differences with respect to bulk, ($\delta\mu_v(z*)$, in units of k_BT, with $\beta = 1/k_BT$) and normalized by r^2. As discussed in the text, comparison of the three sets of $\delta\mu_v(z*)$ reveals that shape and orientation dramatically change the solvation free energy at the interface, as well as its size dependence. The continued lines are the $\delta\mu_v(z*)$ values predicted with the S.O.S. model.

adsorption, while a positive value means that adsorption is disfavored.

The most evident result is that changing the shape and/or orientation induces large variations in the adsorption free energies, much larger by up to an order of magnitude than a change in the volume. For example, for a V-brick of 3.5 Å of equivalent radius, decreasing the volume to 2.5 Å radius reduces $\beta\delta\mu_v(z^*)/r^2$ by $\sim$ 0.04 $k_BT/Å^2$, while changing its orientation to H-brick by $\sim$ 0.3 $k_BT/Å^2$. Moreover, depending on the shape and orientation, the size-dependence (i.e. volume changes) of $\delta\mu_v(z^*)$ is different: increasing size disfavors solvation at the interface most in the case of spheres, less for V-bricks, while it even becomes favorable (i.e. $\delta\mu_v(z^*)$ decreases with r) for H-bricks. These peculiar behaviors have never been reported for solvation in the bulk, nor for other interfaces. For example, in bulk systems shape effects were found insignificant for small cavities, while orientation effects do not exist due to the isotropic environment.[40] They are observed at metal/water interfaces due to the presence of three interfacial regions (I1-I3), with different properties, in series.

C. The S.O.S. model

To rationalize hydrophobic solvation at metal/water interfaces and take into account shape, orientation and size effects, we propose a minimal theoretical model, the S.O.S. model. This model adopts a different point of view with respect to existing solvation theories: it is not the cavity volume, but the way the solute cavity is distributed among the interfacial layers that matters at the interface. We introduce this idea into eq. 2 by decomposing the free energy of cavity formation into partial free energy terms ($\delta\mu^*_{V_I}(z)$), each of them corresponding to the process to form a portion of the cavity in one specific layer (I1 to I3):

$$\delta\mu_v(z) = \sum_{I=1}^{3} \delta\mu^*_I(z) \qquad (2)$$

The $\delta\mu^*_{V_I}(z)$ terms depend on the statistics of density fluctuations within each layer (in analogy with eq. 1) and on how much of the cavity volume is inscribed in that layer according to:

$$\beta\delta\mu^*_I = -V_I(ln\frac{P^I_V(0)}{P^{bulk}_V(0)})_{V\to 0} \qquad (3)$$

where V_I is the portion of the cavity that extends into the I-th layer, while $(ln\frac{P^I_V(0)}{P^{bulk}_V(0)})_{V\to 0}$ is the logarithm of the probability to form an empty volume in that layer divided

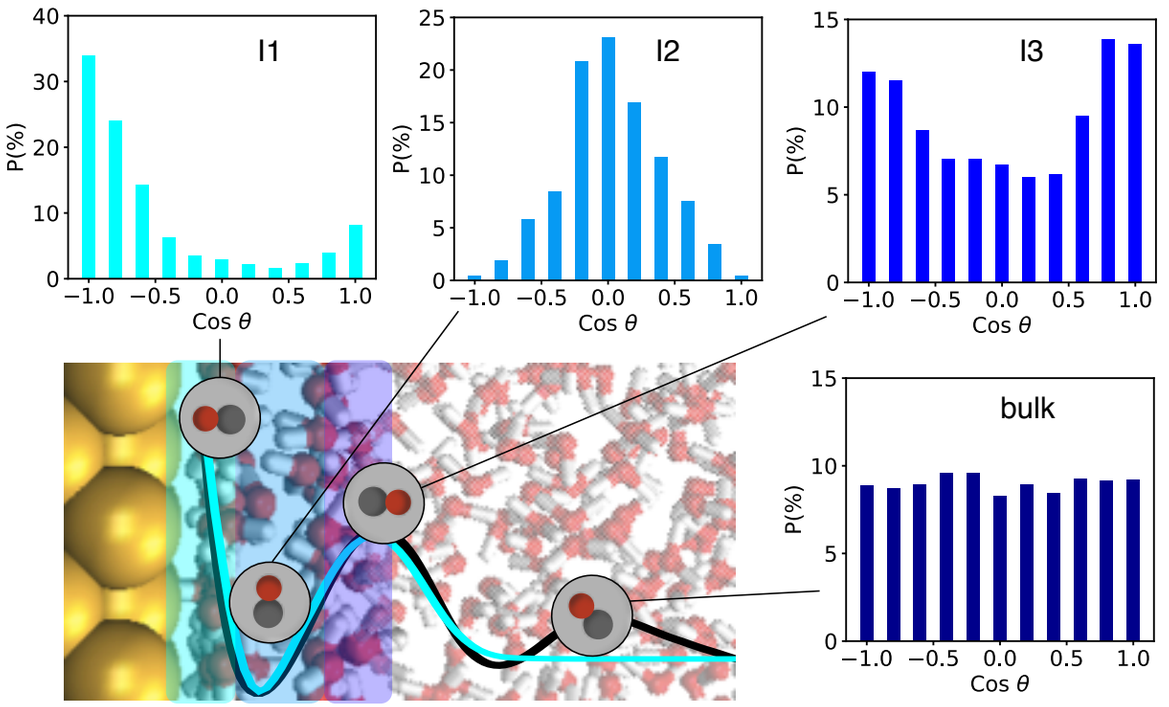

FIG. 3. **From ideal solutes to molecules relevant for electrocatalysis: orientation effects on the adsorption of a CO molecule at the Au(100)/water interface.** The MD snapshot of the interface highlights the three interfacial regions (I1-3), as well as the preferential orientation of CO in each region. The black curve is the adsorption free energy profile of CO, previously computed with the umbrella sampling technique,[15] while the cyan curve is the profile obtained for the CO cavity with the S.O.S. model (see methods for details). The bar plots show the distribution of the cosine of the angle formed between the CO bond vector and the normal to the surface in each region. Cos $\theta = 0$ corresponds to a CO molecule parallel to the surface, while cos $\theta = 1$ to a CO molecule perpendicular to the surface.

by the value in the bulk, per unitary volume (therefore it has the units of an inverse volume). The hypothesis at the heart of the S.O.S. model is that, even though the cavity formation process at the interface is spatially inhomogeneous, it can be approximated as a weighted sum of partial cavity formation processes within each interfacial region (I1-I3), which are spatially homogeneous.

The $(ln\frac{P_V^I(0)}{P_V^{bulk}(0)})_{V\to 0}$ ratios for the interfacial region I2 and I3 have been quantified in this work by fitting the free energy curves of Fig. 2B with eqs. 2-3. We determined $-(ln\frac{P_V^2(0)}{P_V^{bulk}(0)})_{V\to 0} = -18.1$ nm^{-3} for I2 and $-(ln\frac{P_V^3(0)}{P_V^{bulk}(0)})_{V\to 0} = 16.8$ nm^{-3} for I3, i.e. cavity formation is favorable in I2 with respect to bulk, while it is unfavorable in I3. The results from the S.O.S. model are presented as continued line in Fig. 2B. The model nicely reproduces the solvation free energy variations as a function of shape, orientation and size. In the case of the I2 region, we further confirmed that $-(ln\frac{P_V^I(0)}{P_V^{bulk}(0)})_{V\to 0}$ is a constant value for a set of other 15 solutes (on top of the ones analysed in fig.2) of cylindrical and orthorhombic shape, for which we obtained $-(ln\frac{P_V^2(0)}{P_V^{bulk}(0)})_{V\to 0} = -18.1 \pm 1.9$ nm^{-3}. We checked that the same value is obtained if $-(ln\frac{P_V^2(0)}{P_V^{bulk}(0)})_{V\to 0}$ is determined by the probability to form cavities of decreasing volumes (all inscribed within in the I2 region), divided by the cavity volume. We also carefully checked in a previous study[15] that the linear scaling between solvation free energy and cavity volume is preserved at the interface at least until a cavity radius of ∼4 Å. This size range covers the cavities formed by the reactive species involved in important electrocatalytic reactions, such as CO_2 reduction (including C2 products), N_2 reduction, small alcohols oxydation and water splitting. Therefore, the present S.O.S. model is relevant to a wide range of electrochemically interesting solutes.

Once validated, the S.O.S. model allows a straightforward rationalization of the shape and orientation effects. H-bricks have the lowest solvation free energy at the metal/water interface because their most stable location corresponds to being mostly solvated within the hydrophobic water-water interface (I2). Here, density fluctuations are maximized and the free energy of cavity formation is consequently minimized. Increasing the

size of H-bricks corresponds to increase the cavity volume formed within I2, making the adsorption at the interface more and more favorable. Instead, increasing the size for spheres and V-bricks requires forming an empty volume not only within I2, but also within I3, where creating a cavity costs more than in the bulk. Therefore, the adsorption is most favorable for small cavities because they are inscribed within I2, while it becomes less favorable with increasing size. In particular, for the spheres, it even becomes unfavorable for $r \sim 3.0$ Å, because increasing the radius of the sphere makes the partial cavity-volume in I3 larger than that in I2. For the V-bricks the free energy reaches saturation because elongating the longest edge from an equivalent radius of 2.0 Å to 3.0 Å requires forming all the additional empty volume in I3. However, increasing beyond $r = 3.0$ Å, the additional empty volume is formed in the bulk-like region (beyond I3), while the partial volumes in I2 and I3 do not change anymore.

D. Implications for electrocatalysis: orientation and shape matter

In the following, we switch from idealized solutes (i.e. cavities) to realistic molecules in order to test the impact of the observed effects on solutes that are of practical interest for electrocatalysis. We focus, as an example, on how the orientation changes during the adsorption of a CO molecule. This is expected to exhibit the behavior of H/V-bricks. The adsorption free energy profile for the CO molecule was previously computed with the umbrella sampling technique and is reported in Fig. 3 together with a MD snapshot illustrating the preferential orientation of CO when it travels across the distinct interfacial regions. We also computed the adsorption free energy profile for the CO cavity with the S.O.S. model, as reported in cyan in the figure. For the model, the size of the CO cavity was estimated in a previous work,[15] while we determined the preferred orientation from the CO orientation distribution in each interfacial region, as obtained from the umbrella sampling simulations (vide infra). The good agreement between the two profiles provides a further validation of the S.O.S. model.Orientation distributions of the angle formed between the CO molecule (CO bond vector) and the normal to the Au surface are shown in bar plots in the figure. Going from the bulk to the surface, the molecule undergoes precise changes in preferential orientation that are well rationalized by the S.O.S. model. While no preferential orientation is observed in the isotropic bulk region, the CO molecule prefers to orient perpendicular to the surface when traveling across the I3 region. This is to minimize the cavity-volume formed within I3, where cavity formation is disfavored with respect to the adjacent I2 and bulk regions. On the contrary, when located in I2, CO prefers to lay parallel to the surface in order to maximize the cavity-volume formed within this region where density fluctuations are maximized. Finally, the orientation switches again to perpendicular when the molecule penetrates the water adlayer and access the I1 region, in order to minimize the perturbation on the adlayer structure. In the preferred perpendicular orientation assumed by CO in I1 and I3, the oxygen atom systematically points away from the hydrophobic water-water interface (i.e. I2), where the H-Bonding capability of water is low. In the case of I1, the vertical orientation is further stabilized by CO-gold interactions. This result, together with the theoretical experiment of Fig. 2, has an interesting implication for theoretical electrocatalysis, as well as for the success of predictions based on volcano analyses: the orientation that a molecule has to assume in order to adsorb on the metal surface is a crucial parameter, which produces the largest free energy contribution from solvation to the adsorption of planar and linear molecules. This effect has been so far systematically overlooked by static DFT calculations using implicit solvation models.

CONCLUSIONS

We uncovered unexpectedly large effects of the shape and orientation of hydrophobic and amphiphilic molecules on their adsorption free energy, due to the atypical solvation properties of metal/water interfaces. These effects exceed by up to an order of magnitude the already known effects of size and position, which were reported to be sufficiently large to potentially tune the selectivity and rate of e.g. some CO_2 and N_2 reduction pathways.[18] Therefore, tuning shape and orientation effects could open promising avenues for controlling interfacial reactivity, once fully understood.

Toward this goal, we here identified the molecular origin of these peculiar behaviors and proposed a minimal theoretical model, the S.O.S. model, that allows to capture and rationalize size, orientation and shape effects. The model is specific for the cavity-formation contribution to the solvation free energy, which is the dominant contribution for hydrophobic and amphiphilic molecules.[35] In order to have a more complete view, the S.O.S. model can be directly combined with the thermodynamic cycle that we introduced in refs.[18,35] in cases where the additional contribution from attractive interactions formed by the solute is expected to be relevant. With this combination, it will be possible to apply the S.O.S. model even to rationalize the adsorption behavior of some ions, e.g. Cl^-, which was found to be dictated by the cavity formation contribution despite their hydrophilic nature.[16,48]

The main idea introduced in the S.O.S. model is that solvation at metal/water interfaces is determined by (i) the way the solute cavity is distributed among the distinct hydrophilic/hydrophobic interfacial regions formed close to the metal and by (ii) how water density fluctuations change in each region. Both parameters are highly tunable. The first can be tuned by playing with

the shape of the reactive molecules, their size and the way the molecule adsorb on the surface (e.g. preferred orientation). The second is instead tuned by the nature and symmetry of the metal surface and/or the electrolyte composition. For example, recent studies have shown that the hydrophobicity of metal/water interfaces can be regulated by changing metal (e.g. Au *vs* Pt[15]) or by changing surface topology (e.g. different facets of the same metal[34]). It can be even boosted by functionalizing a metal surface with organic polymers, which can result in e.g. a substantial increase in the efficiency of CO_2 electrochemical reduction to ethylene on Cu.[20] Furthermore, molecules adsorbed at the interface during electrochemical processes are expected to modulate the properties of interfacial water, and therefore solvation free energies.The ideas introduced in the S.O.S. model provide a framework to understand such effects in future studies, connecting changes in interface architecture to changes in the properties of the distinct interfacial regions and ultimately to changes in solvation free energies and reactivity.

METHODS

The numerical results on cavity formation free energies have been obtained from a previously performed[15] MD simulation of a Au(100)-water interface, by evaluating the probability, $P_v(0)$, that zero water oxygen centers are found within probing volumes of different shape (spheres and bricks), volume, orientation and distance from the surface. $\Delta\mu_v$ was then obtained from $P_v(0)$ by means of eq.1. The classical MD simulation was performed with the constant potential method (at a fixed applied potential of 0V, corresponding to the point of zero charge of the model) as implemented in the MetalWalls code,[49] over a water slab of 3,481 molecules between two planar Au(100) electrodes (of five layers, 162 Au atoms each). We checked in previous studies that the results on cavity formation free energies are stable with respect to the choices in the computational method, e.g. surface parameters such as surface metallicity and applied potential.[15,50]Two- dimensional periodic boundary conditions were employed, with a simulation box of Lx = Ly = 36.63 Å, and Lz = 78.6 Å. Water was described with the SPC/E[51] model, while Lennard-Jones parameters introduced by Heinz et al.[52] were adopted for Au(100). The choice of a classical force field to describe the metal-water interface can lead to some short-comings on the fine details of the interfacial molecular arrangement. However, the interfacial water structuring close to the metal is preserved and also observed in ab-initio MD.[16,43]After equilibration, a production run of 80 ns, collected with a timestep of 2 fs (NVT, T = 298 K) was used for the analysis. More details can be found in Ref. 15.

The umbrella sampling calculation of the CO adsorption profile along the vertical distance between the CO center of mass and the water adlayer was accomplished in a previous study[15] by using the open-source PLUMED library, version 2.5.[53] Six calculations were performed at regular intervals of z values. The force field parameters from Ref. 54 were used for CO. The orientational distribution of the CO molecule was evaluated for each point of the umbrella sampling by computing the angle between the CO bond vector and the normal to the Au surface.

ACKNOWLEDGMENTS

This work is funded by the European Research Council (ERC, ELECTROPHOBIC, Grant Agreement No. 101077129).

AUTHOR DECLARATIONS

Conflict of interest

The authors have no conflicts to disclose.

DATA AVAILABILITY STATEMENT

The data that support the findings of this study are available from the corresponding author. Typical Input files have been deposited in Zenodo (https://doi.org/10.5281/zenodo.4467959) and GitLab https://gitlab.com/ampere2/serva.

[1]S. Nitopi, E. Bertheussen, S. B. Scott, X. Liu, A. K. Engstfeld, S. Horch, B. Seger, I. E. L. Stephens, K. Chan, C. Hahn, J. K. Nørskov, T. F. Jaramillo, and I. Chorkendorff, "Progress and perspectives of electrochemical co2 reduction on copper in aqueous electrolyte," Chem. Rev. **119**, 7610–7672 (2019).
[2]G. Marcandalli, A. Goyal, and M. T. Koper, "Electrolyte effects on the faradaic efficiency of co2 reduction to co on a gold electrode," ACS catal. **11**, 4936–4945 (2021).
[3]B. A. Rosen, A. Salehi-Khojin, M. R. Thorson, W. Zhu, D. T. Whipple, P. J. Kenis, and R. I. Masel, "Ionic liquid–mediated selective conversion of co2 to co at low overpotentials," Science **334**, 643–644 (2011).
[4]S. Hanselman, M. T. Koper, and F. Calle-Vallejo, "Computational comparison of late transition metal (100) surfaces for the electrocatalytic reduction of co to c2 species," ACS Energy Lett. **3**, 1062–1067 (2018).
[5]T. K. Todorova, M. W. Schreiber, and M. Fontecave, "Mechanistic understanding of co2 reduction reaction (co2rr) toward multicarbon products by heterogeneous copper-based catalysts," ACS Catal. **10**, 1754–1768 (2020).
[6]J. T. Feaster, C. Shi, E. R. Cave, T. Hatsukade, D. N. Abram, K. P. Kuhl, C. Hahn, J. K. Nørskov, and T. F. Jaramillo, "Understanding selectivity for the electrochemical reduction of carbon dioxide to formic acid and carbon monoxide on metal electrodes," ACS Catal. **7**, 4822–4827 (2017).
[7]F. Abild-Pedersen, J. Greeley, F. Studt, J. Rossmeisl, T. R. Munter, P. G. Moses, E. Skúlason, T. Bligaard, and J. K.

Nørskov, "Scaling properties of adsorption energies for hydrogen-containing molecules on transition-metal surfaces," Phys. Rev. Lett. **99**, 016105 (2007).
[8]A. Nilsson, L. G. Pettersson, and J. Norskov, *Chemical bonding at surfaces and interfaces* (Elsevier, 2011).
[9]F. Calle-Vallejo, J. I. Martínez, J. M. García-Lastra, J. Rossmeisl, and M. T. M. Koper, "Physical and chemical nature of the scaling relations between adsorption energies of atoms on metal surfaces," Phys. Rev. Lett. **108**, 116103 (2012).
[10]D. Bao, Q. Zhang, F.-L. Meng, H.-X. Zhong, M.-M. Shi, Y. Zhang, J.-M. Yan, Q. Jiang, and X.-B. Zhang, "Electrochemical reduction of n2 under ambient conditions for artificial n2 fixation and renewable energy storage using n2/nh3 cycle," Adv. Mater. **29**, 1604799 (2017).
[11]F. Luo, A. Roy, L. Silvioli, D. A. Cullen, A. Zitolo, M. T. Sougrati, I. C. Oguz, T. Mineva, D. Teschner, S. Wagner, *et al.*, "P-block single-metal-site tin/nitrogen-doped carbon fuel cell cathode catalyst for oxygen reduction reaction," Nat. Mater **19**, 1215–1223 (2020).
[12]A. J. Garza, A. T. Bell, and M. Head-Gordon, "Mechanism of co2 reduction at copper surfaces: Pathways to c2 products," ACS Catal. **8**, 1490–1499 (2018).
[13]M. R. Singh, J. D. Goodpaster, A. Z. Weber, M. Head-Gordon, and A. T. Bell, "Mechanistic insights into electrochemical reduction of co2 over ag using density functional theory and transport models," Proc. Natl. Acad. Sci. **114**, E8812–E8821 (2017).
[14]O. Cheong, T. Bornhake, X. Zhu, and M. H. Eikerling, "Stay hydrated! impact of solvation phenomena on the co2 reduction reaction at pb (100) and ag (100) surfaces," ChemSusChem , e202300885 (2023).
[15]A. Serva, M. Salanne, M. Havenith, and S. Pezzotti, "Size dependence of hydrophobic hydration at electrified gold/water interfaces," Proc. Natl. Acad. Sci. **118**, e2023867118 (2021).
[16]S. R. Alfarano, S. Pezzotti, C. J. Stein, Z. Lin, F. Sebastiani, S. Funke, C. Hoberg, I. Kolling, C. Y. Ma, K. Mauelshagen, *et al.*, "Stripping away ion hydration shells in electrical double-layer formation: Water networks matter," Proc. Natl. Acad. Sci. **118**, e2108568118 (2021).
[17]N. Dubouis, A. Serva, R. Berthin, G. Jeanmairet, B. Porcheron, E. Salager, M. Salanne, and A. Grimaud, "Tuning water reduction through controlled nanoconfinement within an organic liquid matrix," Nat. Catal. **3**, 656–663 (2020).
[18]A. Serva, M. Havenith, and S. Pezzotti, "The role of hydrophobic hydration in the free energy of chemical reactions at the gold/water interface: Size and position effects," J. Chem. Phys. **155**, 204706 (2021).
[19]P. Li, Y. Jiang, Y. Hu, Y. Men, Y. Liu, W. Cai, and S. Chen, "Hydrogen bond network connectivity in the electric double layer dominates the kinetic ph effect in hydrogen electrocatalysis on pt," Nat. Catal. **5**, 900–911 (2022).
[20]H.-Q. Liang, S. Zhao, X.-M. Hu, M. Ceccato, T. Skrydstrup, and K. Daasbjerg, "Hydrophobic copper interfaces boost electroreduction of carbon dioxide to ethylene in water," ACS Catal. **11**, 958–966 (2021).
[21]N. Singh and C. T. Campbell, "A simple bond-additivity model explains large decreases in heats of adsorption in solvents versus gas phase: A case study with phenol on pt(111) in water," ACS Catal. **9**, 8116–8127 (2019).
[22]P. Clabaut, B. Schweitzer, A. W. Götz, C. Michel, and S. N. Steinmann, "Solvation free energies and adsorption energies at the metal/water interface from hybrid quantum-mechanical/molecular mechanics simulations," J. Chem. Theory Comput. **16**, 6539–6549 (2020).
[23]H. H. Kristoffersen and K. Chan, "Towards constant potential modeling of co-co coupling at liquid water-cu(100) interfaces," J. Catal. **396**, 251–260 (2021).
[24]S. Sakong and A. Groß, "The electric double layer at metal-water interfaces revisited based on a charge polarization scheme," J. Chem. Phys. **149**, 084705 (2018).
[25]A. Bagger, L. Arnarson, M. H. Hansen, E. Spohr, and J. Rossmeisl, "Electrochemical co reduction: A property of the electrochemical interface," J. Am. Chem. Soc. **141**, 1506–1514 (2019).
[26]K. Jiang, R. B. Sandberg, A. J. Akey, X. Liu, D. C. Bell, J. K. Nørskov, K. Chan, and H. Wang, "Metal ion cycling of cu foil for selective c–c coupling in electrochemical co2 reduction," Nat. Catal. **1**, 111–119 (2018).
[27]J. Le, M. Iannuzzi, A. Cuesta, and J. Cheng, "Determining potentials of zero charge of metal electrodes versus the standard hydrogen electrode from density-functional-theory-based molecular dynamics," Phys. Rev. Lett. **119**, 016801 (2017).
[28]R. Khatib, A. Kumar, S. Sanvito, M. Sulpizi, and C. S. Cucinotta, "The nanoscale structure of the pt-water double layer under bias revealed," Electrochim. Acta **391**, 138875 (2021).
[29]A. Groß and S. Sakong, "Ab initio simulations of water/metal interfaces," Chem. Rev. **122**, 10746–10776 (2022).
[30]S. Surendralal, M. Todorova, M. W. Finnis, and J. Neugebauer, "First-principles approach to model electrochemical reactions: Understanding the fundamental mechanisms behind mg corrosion," Phys. Rev. Lett. **120**, 246801 (2018).
[31]C. Zhang, T. Sayer, J. Hutter, and M. Sprik, "Modelling electrochemical systems with finite field molecular dynamics," J. Phys. Energy **2**, 032005 (2020).
[32]L. Scalfi, M. Salanne, and B. Rotenberg, "Molecular simulation of electrode-solution interfaces," Annu. Rev. Phys. Chem. **72**, 189–212 (2021).
[33]L. J. Ahrens-Iwers, M. Janssen, S. R. Tee, and R. H. Meißner, "Electrode: An electrochemistry package for atomistic simulations," J. Chem. Phys. **157** (2022).
[34]D. T. Limmer, A. P. Willard, P. Madden, and D. Chandler, "Hydration of metal surfaces can be dynamically heterogeneous and hydrophobic," Proc. Natl. Acad. Sci. **110**, 4200–4205 (2013).
[35]S. Pezzotti, F. Sebastiani, E. P. van Dam, S. Ramos, V. Conti Nibali, G. Schwaab, and M. Havenith, "Spectroscopic fingerprints of cavity formation and solute insertion as a measure of hydration entropic loss and enthalpic gain," Angew. Chem. Int. Ed. **134**, e202203893 (2022).
[36]D. Chandler, "Interfaces and the driving force of hydrophobic assembly." Nature **437**, 640–647 (2005).
[37]K. Lum, D. Chandler, and J. D. Weeks, "Hydrophobicity at small and large length scales," J. Phys. Chem. B **103**, 4570–4577 (1999).
[38]S. N. Jamadagni, R. Godawat, and S. Garde, "Hydrophobicity of proteins and interfaces: Insights from density fluctuations," Annu. Rev. Chem. Biomol. Eng. **2**, 147–171 (2011).
[39]E. Gallicchio, M. Kubo, and R. M. Levy, "Enthalpy- entropy and cavity decomposition of alkane hydration free energies: Numerical results and implications for theories of hydrophobic solvation," J. Phys. Chem. B **104**, 6271–6285 (2000).
[40]N. Ansari, A. Laio, and A. Hassanali, "Spontaneously forming dendritic voids in liquid water can host small polymers," J. Phys. Chem. Lett. **10**, 5585–5591 (2019).
[41]V. Hande and S. Chakrabarty, "Size-dependent order–disorder crossover in hydrophobic hydration: Comparison between spherical solutes and linear alcohols," ACS Omega **7**, 2671–2678 (2022).
[42]A. P. Willard, S. K. Reed, P. A. Madden, and D. Chandler, "Water at an electrochemical interface - a simulation study," Faraday Discuss. **141**, 423–441 (2009).
[43]C.-Y. Li, J.-B. Le, Y.-H. Wang, S. Chen, Z.-L. Yang, J.-F. Li, and J. Cheng, "In situ probing electrified interfacial water structures at atomically flat surfaces," Nat. Mater. **18**, 697–701 (2019).
[44]S. Schnur and A. Groß, "Properties of metal–water interfaces studied from first principles," New J. Phys. **11**, 125003 (2009).
[45]L. Scalfi, T. Dufils, K. G. Reeves, B. Rotenberg, and M. Salanne, "A semiclassical thomas–fermi model to tune the metallicity of electrodes in molecular simulations," J. Chem. Phys. **153** (2020).
[46]J.-X. Zhu, J.-B. Le, M. T. Koper, K. Doblhoff-Dier, and J. Cheng, "Effects of adsorbed oh on pt (100)/water interfacial structures and potential," J. Phys. Chem. C **125**, 21571–21579

(2021).
[47]G. Pireddu, L. Scalfi, and B. Rotenberg, "A molecular perspective on induced charges on a metallic surface," J. Chem. Phys. **155** (2021).
[48]S. Pezzotti, A. Serva, C. J. Stein, and M. Havenith, *Encyclopedia of Solid-Liquid Interfaces (First Edition)* (Elsevier, 2024) pp. 66–80.
[49]A. Marin-Laflèche, M. Haefele, L. Scalfi, A. Coretti, T. Dufils, G. Jeanmairet, S. K. Reed, A. Serva, R. Berthin, C. Bacon, S. Bonella, B. Rotenberg, P. A. Madden, and M. Salanne, "Metalwalls: A classical molecular dynamics software dedicated to the simulation of electrochemical systems," J. Open Source Softw. **5**, 2373 (2020).
[50]A. Serva, L. Scalfi, B. Rotenberg, and M. Salanne, "Effect of the metallicity on the capacitance of gold–aqueous sodium chloride interfaces," J. Chem. Phys. **155**, 044703 (2021).
[51]H. J. C. Berendsen, J. R. Grigera, and T. P. Straatsma, "The missing term in effective pair potentials," J. Phys. Chem. **91**, 6269–6271 (1987).
[52]H. Heinz, R. A. Vaia, B. L. Farmer, and R. R. Naik, "Accurate simulation of surfaces and interfaces of face-centered cubic metals using 12-6 and 9-6 lennard-jones potentials," J. Phys. Chem. C **112**, 17281–17290 (2008).
[53]G. A. Tribello, M. Bonomi, D. Branduardi, C. Camilloni, and G. Bussi, "Plumed 2: New feathers for an old bird," Comput. Phys. Commun **185**, 604 – 613 (2014).
[54]I. Poudyal and N. P. Adhikari, "Temperature dependence of diffusion coefficient of carbon monoxide in water: A molecular dynamics study," J. Mol. Liq. **194**, 77 – 84 (2014).